Environment. Technology. Resources. Rezekne, Latvia
Proceedings of the 16th International Scientific and Practical Conference 2025. Volume IV, 489-495

The Impact of CO_2 Laser Treatment on Graphene-Modified KM2-440 Ballistic Kevlar Fabric and Its Property Changes

Jēkabs Lapa
Riga Technical University
Rezekne Academy
Rēzekne, Latvia
jekabs.lapa@gmail.com

Imants Adijāns
Riga Technical University
Rezekne Academy
Rēzekne, Latvia
imants.adijans@rta.lv

Silvija Kukle
Riga Technical University
Riga, Latvia
Silvija.Kukle@rtu.lv

Lyubomir Lazov
Riga Technical University
Rezekne Academy
Rēzekne, Latvia
lyubomir.lazov@rta.lv

Ieva Baķe
Riga Technical University
Riga, Latvia
Ieva.Bake@rtu.lv

Uģis Briedis
Riga Technical University
Riga, Latvia
uģis.briedis@rtu.lv

***Abstract* — This study investigates the laser marking of graphene-modified KM2-440 ballistic Kevlar fabric, exploring how different laser parameters affect its properties. A 1x4 matrix was marked on the fabric using the SUNTOP ST-CC9060 laser system, with each square measuring 30 mm in length and 40 mm in width. Our adjustments to the laser marking parameters encompassed variations in speed and power. Specifically, the speed ranged from 100 mm/s to 150 mm/s, while the power varied between 8.5% and 8.8%. A constant step size (Δx) of 0.08 mm was maintained for all markings. These parameter variations were studied to assess their impact on the fabric's mechanical properties, surface roughness, and durability. Advanced testing methods, including the Olympus LEXT OLS5000 3D Measuring Laser Microscope, were employed to examine the correlation between laser marking parameters and the changes in the fabric's ballistic performance. The findings provide significant insights into the effects of laser processing on the structural integrity and performance of graphene-modified Kevlar fabrics. This research not only contributes to optimizing laser marking parameters for enhanced fabric durability but also offers valuable knowledge on how graphene incorporation affects the ballistic characteristics of Kevlar in the context of laser treatment.**

Keywords* — *laser marking, ballistic Kevlar fabric, graphene-modified,* CO_2 *Laser, laser parameters, mechanical properties, surface roughness.

1. Introduction

In the rapidly advancing field of materials processing, laser technologies have emerged as powerful tools for modifying and enhancing material properties [1]. Over the past decades, lasers have revolutionized traditional processing techniques, offering unparalleled precision, efficiency, and adaptability across various industries, including aerospace, defense, and protective material engineering[2]. Among the numerous laser applications, laser marking and surface modification have gained increasing attention due to their potential to improve material durability [3], mechanical properties, and functional performance.

Recent research has demonstrated the effectiveness of laser treatment in modifying polymeric and composite materials [4], making it a promising approach for enhancing ballistic textiles. CO_2 lasers, in particular, have been widely used for surface structuring and controlled material ablation, leading to alterations in mechanical, thermal, and optical properties [5, 6].

In comparison to conventional mechanical treatments, laser processing offers a contactless, highly controllable, and non-destructive method for modifying ballistic fabrics while preserving their flexibility and structural integrity [7].

Online ISSN 2256-070X
https://doi.org/10.17770/etr2025vol4.8389

The integration of graphene into Kevlar-based fabrics represents a novel advancement in the development of next-generation ballistic materials [7]. Graphene, due to its exceptional mechanical strength, electrical conductivity, and thermal stability, has been explored as a reinforcement material in composite applications [8]. However, the challenge remains in effectively incorporating graphene into ballistic Kevlar fabrics while maintaining uniform dispersion and adhesion to the fiber structure [8]. Laser-assisted processing has emerged as a potential technique for enhancing the interaction between graphene and Kevlar fabrics, improving overall material performance.

Current studies on laser-treated graphene-reinforced composites [9] have predominantly focused on metals and rigid polymer structures, with limited research on Kevlar-based ballistic fabrics. The impact of CO_2 laser marking [10] on the microstructural and mechanical properties of graphene-modified KM2-440 ballistic Kevlar fabric remains largely unexplored. By understanding how laser parameters such as power and scanning speed affect the fabric's structural integrity [11], surface roughness, and durability, this study seeks to bridge the knowledge gap in laser-assisted modification of ballistic materials [12].

The objective of this research is to investigate the effects of CO_2 laser processing on graphene-modified KM2-440 ballistic Kevlar fabric, analyzing how different laser parameters influence material properties. A 1×4 matrix was laser-marked using the SUNTOP ST-CC9060 laser system, with varying power (8.5%–8.8%) and scanning speed (100 mm/s–150 mm/s), while maintaining a constant step size of 0.08 mm. To evaluate the laser-induced modifications, advanced characterization techniques, including the Olympus LEXT OLS5000 3D Measuring Laser Microscope, were utilized to assess surface roughness, microstructural changes, and potential improvements in ballistic performance.

The findings of this study will contribute to the development of more durable and impact-resistant ballistic materials [13], advancing protective equipment design for military and law enforcement applications [14, 15]. By optimizing laser processing parameters, this research aims to enhance the structural stability and longevity of graphene-enhanced Kevlar fabrics, ultimately leading to stronger, lighter, and more effective protective armor equipment.

II. Materials and Methods

A. Materials Characteristics

This study focused on an experimental examination a graphene-modified para-aramid ballistic fabric.

The technological limitations of laser processing are primarily influenced by the anticipated effects of the process and the inherent structural characteristics of the material being processed [19], alongside the varying properties of both the substrate and the material itself [19]. The fundamental structural component of Kevlar® consists of a backbone composed of para-oriented benzene rings [19], which facilitates the formation of rod like molecular structures, subsequently leading to the formation of liquid crystalline polymers [19].

Kevlar® KM2+ high modulus fibres woven plain weave fabric style 310 is used (Producer SAATI, Italy). 440 dtex thread density 14 cm^{-1} in warp and weft direction. Fabric thickness 0.17mm, areal density 128 g/m2. The longitudinal Young's modulus of the Kevlar® KM2 fibre is 84.62±4.18 GPa, the ultimate strength of 3.88±0.40 GPa with a failure strain of 4.52%±0.37% and diameter measured using a scanning electronic microscope 12 μm [18] The physical dimensions of the specimen were 100 × 100 mm, with a single-layer thickness of approximately 0.30 mm.

Prior to experimentation, the Kevlar fabric underwent a thorough surface cleaning procedure, including soaking in acetone (2 hours), washing and drying, to eliminate any surface contaminants and finishing agents [7]. This ensured optimal adhesion of the graphene layer to the fabric surface. Subsequently, graphene nanoplatelets were introduced by fabric dip-coating and followed thermal consolidation [7, 8]. This technique was followed by thermal curing at 60°C for 1 hour to promote strong chemical bonding between the graphene coating and the Kevlar fabric surface [7], thereby enhancing the mechanical and electrical properties of the fabric [7, 8].

B. Laser setup

The laser setup used in the experiments was based on the CO_2 Suntop ST-CC9060 system, as shown in Figure 1. Operating with a wavelength of 10640 nm, this continuous-wave (CW) laser system is capable of reaching a maximum power of 100 W. The laser's workspace spans 900 x 600 mm, providing a large area for operation. The precision of the system is maintained at 0.02 mm, ensuring high accuracy during the process. The scan speed of the laser can be adjusted from 0 to 1000 mm/s, depending on the specific needs of the experiment. A water-cooling system was employed to maintain the laser's optimal operating temperature. The laser is classified as Class 4 for safety, requiring proper precautions during use.

It supports data formats including Dxf, bmp, and ai for flexible input options. The total power consumption of the system is 1500 W, ensuring sufficient energy for its high-performance capabilities.

Fig. 1. CO_2 SUNTOP ST-CC9060.

Specification for SUNTOP ST-CC9060 is shown in Table I.

TABLE I. PARAMETERS OF SUNTOP ST-CC9060

Parameter	Magnitude, Unit
Wavelength (*λ*)	10640 nm
Max. Power (*P*)	100 W
Operation mode	CW
Workspace	900 x 600 mm
Precision	0,02 mm
Scan speed	0 – 1000mm/s
Laser Safty Class	4
Cooling system	Water cooling
Data formats	Dxf, bmp, ai
Total power	1500 W

C. Microscope setup

To analyze the surface properties and modifications of the Kevlar KM2-440 ballistic fabric specimens, a 3D laser microscope, specifically the Olympus LEXT OLS5000, was employed, as shown in Figure 2. The microscope operated at a magnification of 451x, ensuring a measurement precision of 0.4 µm. The key technical specifications included a numerical aperture (N.A.) of 0.6, a working distance (W.D.) of 1 mm, a focal depth of 1.8 µm, and a focusing spot diameter of 0.82 µm. The device was capable of measuring an area of 640 × 640 µm, allowing for detailed surface analysis of the Kevlar fabric.

Fig. 2. Olympus LEXT OLS5000 3D Measuring Laser Microscope.

E. Experimental Method

Laser marking was conducted on a Graphene-Modified KM2-440 Ballistic Kevlar Fabric sample with dimensions of [180 x 50 mm] using a CO_2 SUNTOP ST-CC9060 laser. The sample surface remained in its original state without additional cleaning or treatment prior to marking. The marking process involved the creation of a single matrix comprising four rows and one marking.

The laser marking parameters were meticulously adjusted, incorporating a speed of 150 mm/s, power ranging from 8.5% to 8.8%, and a constant step size (Δx) of 0.08 mm for all markings. Specifically, for the first marking, power (P) was set to 8.8%, speed (V) to 150 mm/s, and step size (Δx) to 0.08 mm; for the second marking, P = 8.5%, V = 150 mm/s; for the third marking, P = 8.8%, V = 100 mm/s; and for the fourth marking, P = 8.5%, V = 100 mm/s. The experiments were conducted under ambient conditions without the use of assist gases. The laser marking of the Graphene-Modified KM2-440 Ballistic Kevlar Fabric plate was performed by varying two critical parameters: power (P) in watts and scanning speed (V) in mm/s. Figure 3 illustrates the marking schematics utilized in the experiments.

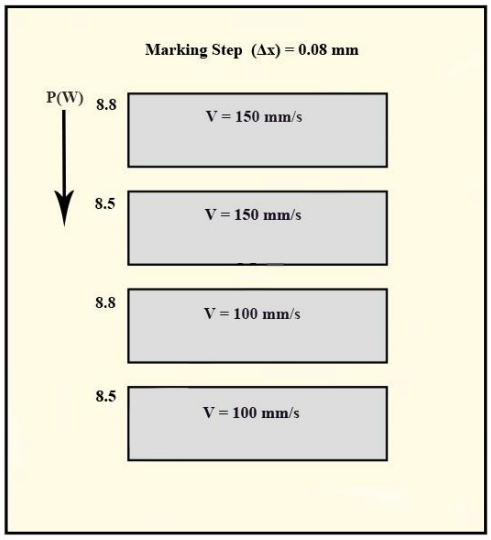

Fig. 3. Laser marking schematics of GRAPHENE-MODIFIED KM2-440 BALLISTIC KEVLAR FABRIC.

In this study, a single matrix was employed, consisting of four rows and one marking, as detailed in Table II. No variations in frequency were introduced. This approach facilitates a comprehensive investigation of the laser marking process, with a particular emphasis on the influence of speed and power settings while maintaining a consistent pulse duration.

TABLE II. CO_2 LASER MARKING PARAMETERS FOR GRAPHENE-MODIFIED KM2-440 BALLISTIC KEVLAR FABRIC

Parameter	Magnitude, Unit
Step size *(Δx)*	0,08 mm
Output Power (*P*)	8.8\8.5\8.8\8.5 %
Scanning Speed (*v*)	150\150\100\100 mm/s
Square Size	30×40 mm

Equation (1) was used to convert the laser power from % to W.

$$P(W) = \frac{P(\%) * P_{max}}{100\%} \quad (1)$$

The computed laser power values, derived from the corresponding percentage settings, are systematically presented in Table III to illustrate the precise power outputs utilized in the experimental process. Additionally, the table includes the corresponding speed values to provide a comprehensive overview of the relationship between power and speed.

TABLE III. POWER AND SPEED CHART

	Test 1	Test 2	Test 3	Test 4
***P* (W)**	8.8	8.5	8.8	8.5
V(mm/s)	150	150	100	100

The contrast factor (K_X) is determined as a percentage value, representing the difference between the unmarked and laser-marked areas [16].

The volume of (K_X) requires assessing the volume of the unmarked region, denoted as (N_f) [17], while the value (N_X) is obtained directly from the laser-marked region. The equation used for this computation is given as follows in Equation (2):

$$K_X = \frac{N_F - N_X}{N_F} \times 100\% \quad (2)$$

To analyze the difference between measured points, a three-dimensional space-based approach is employed. The total difference for the laser-marked region (N_X) is calculated using equation (3):

$$N_x = \sqrt{(\Delta L_x)^2 + (\Delta a_x)^2 + (\Delta b_x)^2} \quad (3)$$

Similarly, the total difference for the unmarked region, (N_f), is expressed in equation (4):

$$N_f = \sqrt{(\Delta L_f)^2 + (\Delta a_f)^2 + (\Delta b_f)^2} \quad (4)$$

In these equations, ΔL, Δa, and Δb represent specific measured variations in the material's response. These values are obtained through analytical evaluation, ensuring precise differentiation between the marked and unmarked areas.

To maintain consistency in contrast assessment, absolute values (K_X)are applied to prevent negative contrast values from affecting result interpretation.

III. RESULTS AND DISCUSSIONS

Surface roughness measurements (Sq, in µm) were conducted on samples processed using varying laser parameters, alongside an unmarked reference surface. Each condition was evaluated at five measurement points to assess surface structure and the influence of processing parameters. The resulting data, including roughness, standard deviation, and percentage change relative to the unmarked surface, are presented in Table IV.

TABLE IV. SURFACE ROUGHNESS SUMMARY (SQ, SD, % CHANGE)

Condition	Roughness (µm)	Std Dev (µm)	Change vs Unmarked (%)
8.8% – 150 mm/s	6.12	0.62	+1.09
8.5% – 150 mm/s	6.20	0.88	+2.39
8.8% – 100 mm/s	5.78	0.69	-4.57
8.5% – 100 mm/s	6.82	0.44	+12.67
Unmarked surface	6.05	0.74	0.00

The unmarked surface exhibited roughness of 6.057 µm, with a standard deviation of 0.746 µm, representing the natural baseline texture of the material without any laser-induced modification.

Among the laser-marked samples:

- At 8.8% power and 150 mm/s, the mean roughness was 6.123 µm, showing a 1.09% increase compared to the unmarked surface.
- At 8.5% power and 150 mm/s, the roughness increased further to 6.201 µm (+2.39%), suggesting that even a slight reduction in power at a constant speed may lead to more significant surface alteration.
- At 8.8% power and 100 mm/s, the roughness decreased to 5.780 µm, a −4.57% change compared to the unmarked baseline. This indicates that slower scanning speed at the same power level may result in a smoother surface morphology.

The most significant increase in roughness was observed at 8.5% power and 100 mm/s, where the surface reached 6.824 µm, corresponding to a 12.67% increase over the unmarked surface. This condition appears to result in the most pronounced topographical modification shown in Figure 4.

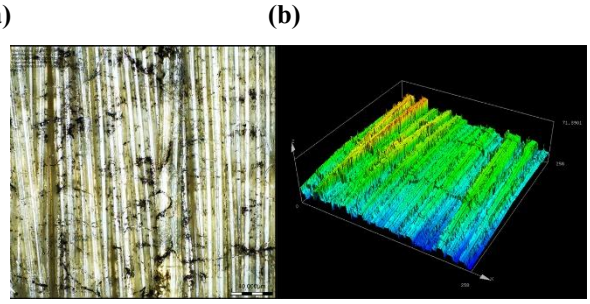

Fig. 4. Surface Morphology of Laser-Marked Graphene-Modified KM2-440 Ballistic Kevlar Fabric at 8.5% Power and 100 mm/s Scanning Speed Showing the Most Pronounced Increase in Surface Roughness Compared to the Unmarked Material.

These findings demonstrate that both laser power and scanning speed are critical roles in determining the final surface characteristics. Notably, the combination of lower power and slower speed have pointed to the highest roughness values, likely due to increased thermal interaction intervals and greater energy deposition per unit area. Conversely, higher power combined with slower scanning speed did not always result in greater roughness, pointing to non-linear relationship influenced by factors such as material absorption threshold and heat dissipation.

Variations in standard deviation across the tested conditions reflect differences in surface consistency. For instance, the 8.5% – 150 mm/s condition exhibited the highest variability, with a standard deviation of 0.882 µm, indicating less consistency in surface texture across the measurement points. In contrast, the 8.5% – 100 mm/s sample showed the most consistent surface, with a lower standard deviation of 0.446 µm, indicating a more homogeneous and consistent surface texture.

In conclusion, the results show that even relatively small changes in laser processing parameters such as slight variations in power or scanning speed—can lead to measurable differences in surface roughness and texture. These differences may significantly affect surface functionality, particularly in materials like Kevlar where surface performance is critical. Therefore, precise control and optimization of laser parameters are essential for ensuring repeatable and application-specific surface properties in laser-marked graphene-modified ballistic materials.

In addition to changes in surface roughness, laser marking also alters the optical properties of the material, particularly surface contrast. Contrast is a factor for the visual detection and readability of the marked features, especially in applications requiring high traceability or optical scanning shown in Figure 5.

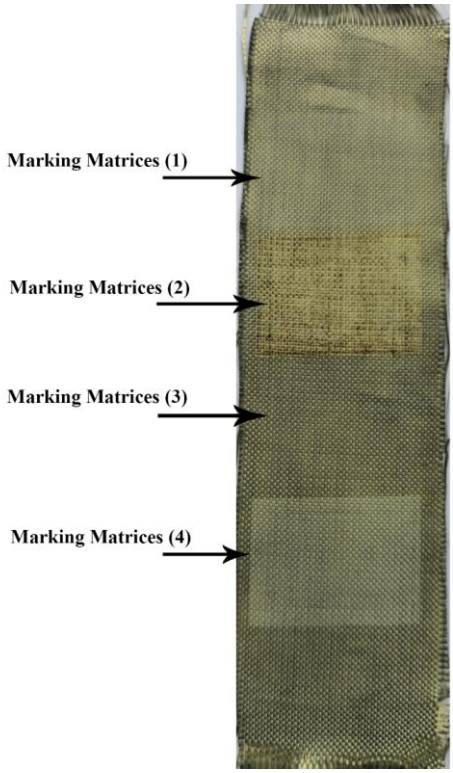

Fig. 5. Laser-Marked Graphene-Modified KM2-440 Kevlar Fabric Showing Four Distinct Marking Matrices (1) – (4).

The image shows a graphene-modified KM2-440 Kevlar fabric with four laser-marked regions labeled (1) through (4). The photo was taken using 8K-resolution camera, clearly capturing the contrast between the marked areas and the surrounding unmarked surface. These visible differences allow for visual evaluation of how laser processing parameters affect surface appearance and marking visibility.

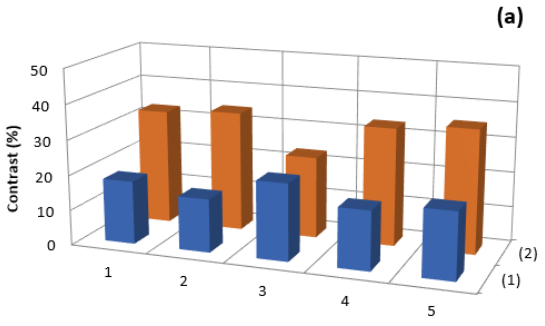

Fig. 6. Contrast Response at Multiple Surface Points on Laser-Marked Matrices (1) and (2).

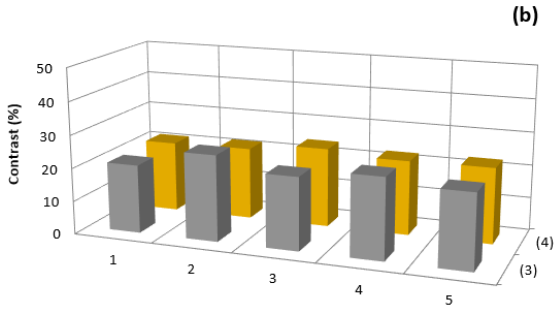

Fig. 7. Contrast Response at Multiple Surface Points on Laser-Marked Matrices (3) and (4).

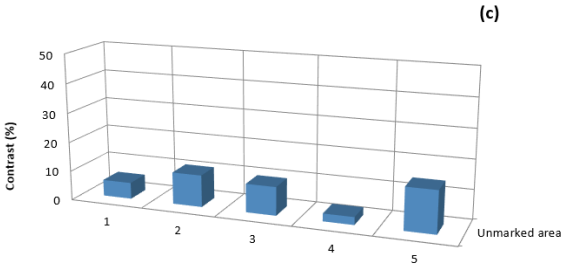

Fig. 8. Contrast Response at Multiple Surface Points on Unmarked Area.

To further evaluate the visual impact of laser processing, contrast levels were analyzed at five distinct surface points across four laser-marked matrices shown in Figure 5, as well as on the unmarked reference area. The calculated contrast values revealed clear differences between treated and untreated zones, indicating that laser parameters significantly influence surface visibility and markings.

The unmarked region exhibited a mean contrast of 33.30%, serving as the baseline for comparison. Among the laser-marked matrices, Matrix (2) shown in Figure 5 demonstrated the highest mean contrast at 50.23%, corresponding to a 50.84% increase over the unmarked surface. This result suggests that the parameter combination used for matrices (2) produced the most optically distinctive surface modification shown in Figure 9.

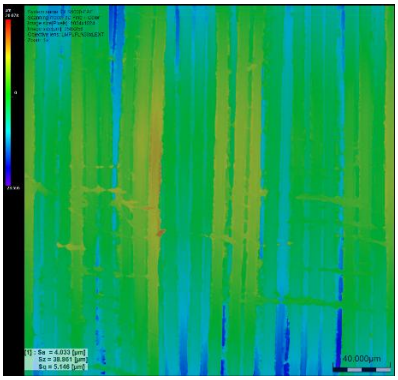

Fig. 9. High-Contrast Surface Modification on Graphene-Modified Kevlar (Matrix 2).

Microscopic examination of Matrix (2) (Figure 9) revealed significant surface alterations, including localized melting and the fusion between the graphene coating and the KM2-440 ballistic Kevlar fabric.

This suggests that the high energy density applied in this region enhanced the interaction between the coating and the substrate, contributing to the observed increase in contrast and altered surface morphology.

The contrast improvements are likely attributable to thermally induced effects, such as microstructural rearrangement, which influence light absorption and reflectivity. These changes highlight the role of thermal interaction in defining the optical response of laser-treated surfaces.

Matrix (1) exhibited a moderate mean contrast of 40.26%, corresponding to a 20.90% increase over the unmarked region. Matrices (3) and (4) showed similar contrast values of 43.88% and 43.45%, equating to 31.77% and 30.48% increases, respectively. These results confirm consistent contrast enhancement across all marked zones, though the effect was most pronounced in Matrix (2).

IV. Conclusions

In this study, we investigated how CO_2 laser treatment affects surface roughness and contrast in graphene-modified KM2-440 ballistic Kevlar fabric. The findings revealed that laser power and scanning speed can significantly alter the fabric's surface characteristics, particularly at low laser power outputs. The highest increase in surface roughness, specifically 12.67%, was observed at a laser power setting of 8.5% combined with a scanning speed of 100 mm/s. These results highlight the importance of precise laser parameter optimization, as excessive laser power can damage the surface structure of fabric-based materials.

References

[1] X. Zhang, Y. Liu, and Z. Wang, "Microstructure and properties of laser cladding CoCrNi-based medium-entropy alloy enhanced by Nb," Journal of Materials Research and Technology, vol. 14, no. 3, pp. 1234-1245, Feb. 2025, doi: 10.1016/j.jmrt.2025.02.100.

[2] S. A. Ahmed, M. Mohsin, and S. M. Z. Ali, "Survey and technological analysis of laser and its defense applications," Defence Technology, vol. 16, no. 1, pp. 1-12, Jan. 2020, doi: 10.1016/j.dt.2020.02.012.

[3] Ł. Łacho, "Recent Advances in Laser Surface Hardening: Techniques, Modeling Approaches, and Industrial Applications," Crystals, vol. 14, no. 8, pp. 726, Aug. 2024, doi: 10.3390/cryst14080726.

[4] S. J. Lim, J. Cheon, and M. Kim, "Effect of laser surface treatments on a thermoplastic PA 6/carbon composite to enhance the bonding strength," Composites A: Applied Science and Manufacturing, vol. 137, pp. 105989, Jun. 2020, doi: 10.1016/j.compositesa.2020.105989.

[5] K. Czyż, J. Marczak, R. Major, A. Mzyk, A. Rycyk, A. Sarzyński, and M. Strzelec, "Selected laser methods for surface structuring of biocompatible diamond-like carbon

layers," Diamond and Related Materials, vol. 68, pp. 44-52, Mar. 2016, doi: 10.1016/j.diamond.2016.01.013.

[6] S. Ravi-Kumar, B. Lies, H. Lyu, and H. Qin, "Laser Ablation of Polymers: A Review," Procedia Manufacturing, vol. 39, pp. 601-608, 2019, doi: 10.1016/j.promfg.2019.06.155.

[7] Kukle, S., Bake, I., & Abele, L. (2024). Graphene-containing para aramid fabric coating via surfactant assisted exfoliation of graphite. Materials Today: Proceedings, 97, 44-51. https://doi.org/10.1016/j.matpr.2023.09.131.

[8] L. Li, M. Zhou, L. Jin, L. Liu, Y. Mo, X. Li, Z. Mo, Z. Liu, S. You, and H. Zhu, "Research Progress of the Liquid-Phase Exfoliation and Stable Dispersion Mechanism and Method of Graphene," Frontiers in Materials, vol. 6, pp. 325, Jun. 2019, doi: 10.3389/fmats.2019.00325.

[9] L. Groo, J. Nasser, L. Zhang, K. Steinke, D. Inman, and H. Sodano, "Laser induced graphene in fiberglass-reinforced composites for strain and damage sensing," Composites Science and Technology, vol. 196, pp. 108367, Jan. 2020, doi: 10.1016/j.compscitech.2020.108367.

[10] M. Ueda, Y. Saitoh, H. Hachisuka, H. Ishigaki, Y. Gokoh, and H. Mantani, "Studies on CO2 laser marking," Applied Surface Science, vol. 42, no. 2, pp. 121-126, Dec. 1990, doi: 10.1016/0143-8166(90)90020-A.

[11] D. Simson and S. Kanmani Subbu, "Effect of Process Parameters on Surface Integrity of LPBF Ti6Al4V," Procedia CIRP, vol. 108, pp. 698-703, Mar. 2022, doi: 10.1016/j.procir.2022.03.111.

[12] S. Wu, P. Sikdar, and G. S. Bhat, "Recent progress in developing ballistic and anti-impact materials: Nanotechnology and main approaches," Defence Technology, vol. 18, no. 6, pp. 1301-1310, Jun. 2022, doi: 10.1016/j.dt.2022.06.007.

[13] S. Wu, P. Sikdar, and G.S. Bhat, Recent progress in developing ballistic and anti-impact materials: Nanotechnology and main approaches. Defence Technology, 2023, 21, pp. 33-61. https://doi.org/10.1016/j.dt.2022.06.007

[14] W. Zou, Recent advancements in ballistic protection - a review. Journal of Student Research, 13(1), 2024. https://doi.org/10.47611/jsrhs.v13i1.5936

[15] J. Shi, H. Li, F. Xu, and X. Tao, Materials in advanced design of personal protective equipment: A review. Materials Today Advances,2021, 12, 100171. https://doi.org/10.1016/j.mtadv.2021.100171

[16] L. Lyubomir, N. Pavels and D. Hristina, "Laser Marking Methods", Technology. Resources, 2015, Volume I, 108-115, pp. 109-112., 2015.

[17] K. McLAREN, XIII—The Development of the CIE 1976 (L* a* b*) Uniform Colour Space and Colour-difference Formula, vol. 92, Journal of the Society of Dyers and Colourists, 1976, pp. 338-341.

[18] B. Sanborn, A. M. Dileonardi, and T. Weerasooriya, "Tensile properties of Dyneema SK76 single fibers at multiple loading rates using a direct gripping method," Journal of Dynamic Behavior of Materials, vol. 1, no. 1, pp. 4-14, Mar. 2014, doi: 10.1007/s40870-014-0001-3.

[19] S. J. Picken, D. Sikkema, H. Boerstoel, and S. Van der Zwaag, "Liquid crystal main-chain polymers for high-performance fibre applications," Liquid Crystals, vol. 38, no. 11-12, pp. 1591-1605, Nov. 2011, doi: 10.1080/02678292.2011.624367.